Supplementary Information

Shape-Adaptive Hydrogel with Dual Antibacterial and Osteogenic Properties for Alveolar Bone Defect Repair

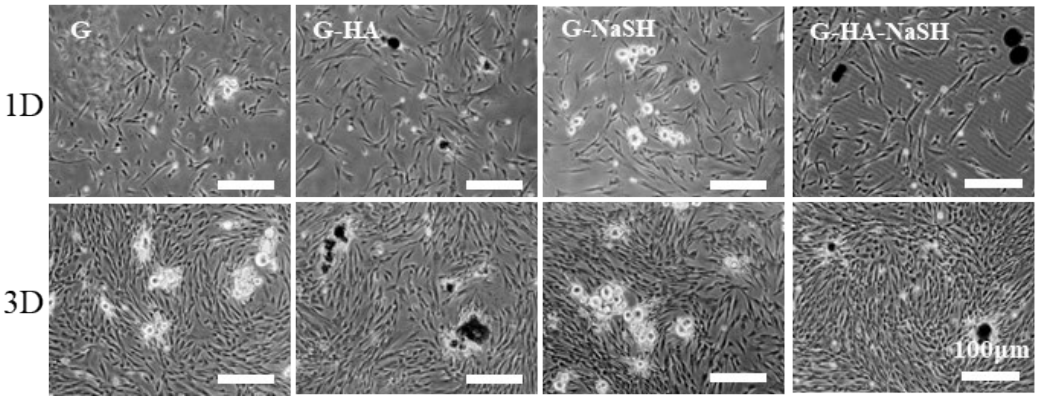

Fig. S1. Bright field microscopy images of cells directly co-cultured with microspheres for 1 and 3 days under an inverted microscope.

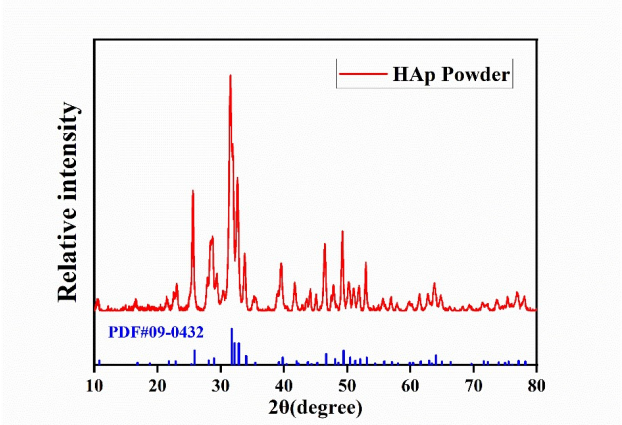

Fig. S2. XRD results of nano-HAP.

Fig. S3. Injectable properties of the hydrogel.

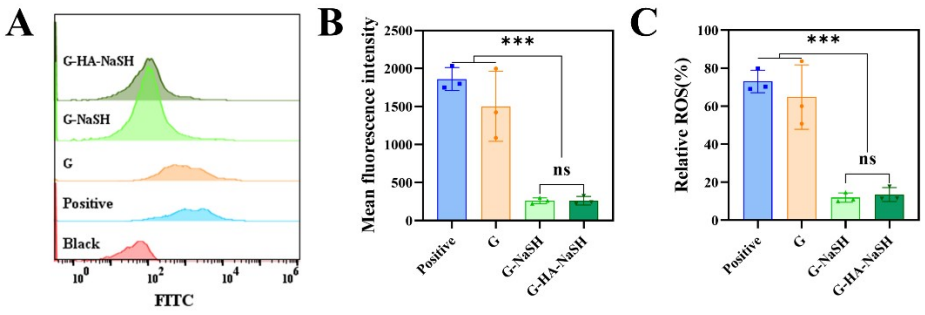

Fig. S4. The ability of hydrogels to clear ROS in vitro. A) The ROS content of BMSCs co-cultured with hydrogels was determined by flow cytometry. B-C) Quantitative results in Figure A. (ns: P>0.05, ***: P<0.001)

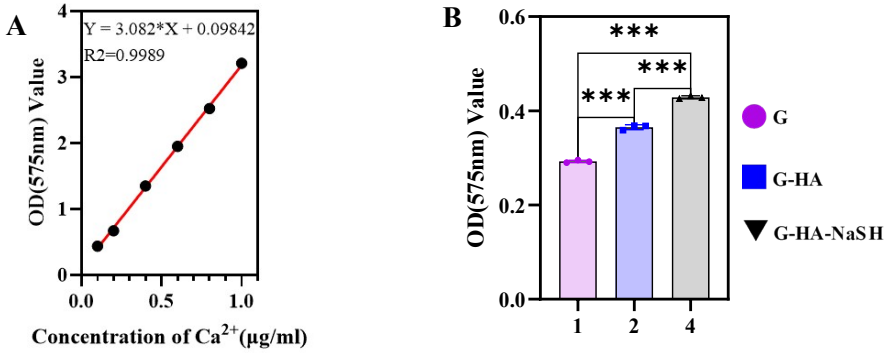

Fig. S5. Standard curve of the calcium ions and the absorbance results. A) Standard curve of the relationship between calcium ions of different concentrations and absorbance; B) Absorbance results. (***: P<0.001)

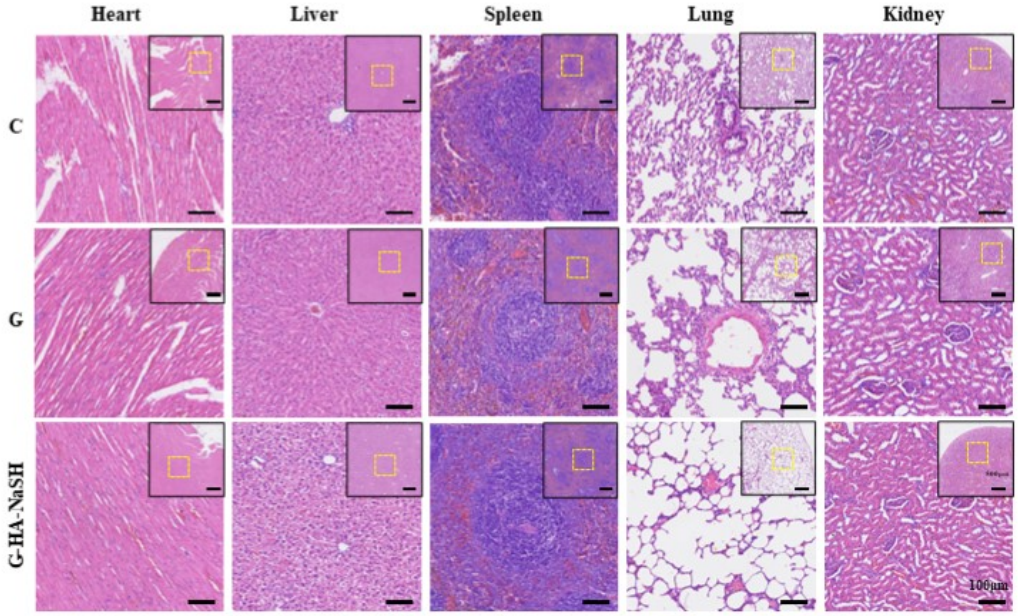

Fig. S6. H&E staining of the internal organs of rats implanted with the hydrogel in the bone defect area for 4 weeks.

Table S1: Sequence of bone formation related gene primers in rats

Gene	Primer sequence
Gapdh	Forward: AAGTTCAACGGCACAGTCAAGG
	Reverse: GACATACTCAGCACCAGCATCAC
Alp	Forward: ACCTGACTGACCCTTCCCTCTC
	Reverse: CAATCCTGCCTCCTTCCACTAGC
Col1a1	Forward: TGGTCCTGCTGGCAAGAATGG
	Reverse: TCTGTCACCTTGTTCGCCTGTC
Runx2	Forward: ACTTCGTCAGCGTCCTATCAGTTC
	Reverse: CCATCAGCGTCAACACCATCATTC

Table S2: Sequence of osteoclast-related gene primers in mice

Gene	Primer sequence
Gapdh	Forward: GCAAATTCAACGGCACAGTCAAG
	Reverse:TCGCTCCTGGAAGATGGTGATG
Rank	Forward:CACTGAGGAGACCACCCAAGG
	Reverse: AGCCACTACTACCACAGAGATGAAG
Rankl	Forward: CCTCCCGCTCCATGTTCCTG
	Reverse: AGTGCTGTCTTCTGATATTCTGTTAGG
Opg	Forward: AGTGAATGCCGAGAGTGTAGAGAG
	Reverse: AGGTCAATGTCTTGGATGATCTTCTTC
Mcsf	Forward: CCAGAAGGAGGACCAGCAAGTG
	Reverse: CCAGCAGGTGGAAGACAGACTC